

Relationships between the degrees of freedom in the affine Gaussian derivative model for visual receptive fields and 2-D affine image transformations, with application to covariance properties of simple cells in the primary visual cortex

Tony Lindeberg

Abstract When observing the surface patterns of objects delimited by smooth surfaces, the projections of the surface patterns to the image domain will be subject to substantial variabilities, as induced by variabilities in the geometric viewing conditions, and as generated by either monocular or binocular imaging conditions, or by relative motions between the object and the observer over time. To first order of approximation, the image deformations of such projected surface patterns can be modelled as local linearizations in terms of local 2-D spatial affine transformations.

This paper presents a theoretical analysis of relationships between the degrees of freedom in 2-D spatial affine image transformations and the degrees of freedom in the affine Gaussian derivative model for visual receptive fields. For this purpose, we first describe a canonical decomposition of 2-D affine transformations on a product form, closely related to a singular value decomposition, while in closed form, and which reveals the degrees of freedom in terms of (i) uniform scaling transformations, (ii) an overall amount of global rotation, (iii) a complementary non-uniform scaling transformation and (iv) a relative normalization to a preferred symmetry orientation in the image domain. Then, we show how these degrees of freedom relate to the degrees of freedom in the affine Gaussian derivative model.

Finally, we use these theoretical results to consider whether we could regard the biological receptive fields in the primary visual cortex of higher mammals as being able to span the degrees of freedom of 2-D spatial affine transformations, based on interpretations of existing neurophysiological experimental results.

Keywords Receptive field · Image transformations · Affine · Covariance · Gaussian derivative · Simple cell

1 Introduction

When viewing a 3-D object in the environment from different distances and different viewing directions, the projected 2-D images on either the retina or the camera sensor will be subject to a substantial variability, as caused by the variability in the viewing conditions (see Figure 1 for illustrations).

To first order of approximation, by approximating the perspective mappings from a smooth local surface patch on the object to any two different perspective images by local linearizations (first-order derivatives), the resulting variability of resulting image data from such multi-view observations of the same surface patch can be modelled in terms of local affine transformations of the form

$$x' = \mathcal{A}x. \quad (1)$$

For simplicity, we have here discarded a possible complementary variability with respect to an added translation vector b in the image domain of the form $x' = \mathcal{A}x + b$, by without essential loss of generality assuming that all the multi-view observations of the same surface patch are focused on the same viewing point P on the 3-D object, and with the origins of the coordinate systems in the image domain also corresponding to the projections of that same fixation point.

A non-trivial, while sometimes overlooked, aspect of visual perception is that we perceive an object in the world as the same, although the 2-D perspective projections of such an object can differ substantially, depending on the viewing distance and the viewing direction of the observer.

A conceptual question that one could then ask is if the ability of perceptual system to derive seemingly stable representations of external objects in the 3-D environment would lead to constraints regarding the variabilities in the shapes

The support from the Swedish Research Council (contract 2022-02969) is gratefully acknowledged.

Computational Brain Science Lab, Division of Computational Science and Technology, KTH Royal Institute of Technology, SE-100 44 Stockholm, Sweden. E-mail: tony@kth.se ORCID: 0000-0002-9081-2170.

Uniform scaling transformations caused by varying the distance between the object and the observer



Rotations in the image plane caused by relative rotations around the optical axis between the object and the observer



Foreshortening transformations caused by varying the viewing direction relative to the object



Fig. 1 Basic types of variabilities in natural image data as caused by geometric image transformations: **(top row)** Uniform scaling transformations caused by varying the distance between the object and the observer. **(middle row)** Rotations in the image domain caused by relative rotations between the object and the observer around the optical axis. **(bottom row)** Foreshortening transformations that lead to non-uniform scaling transformations with the tilt direction (the projection of the surface normal to the image plane) as a preferred orientation in the image plane. Notably, despite these variabilities in the image domain, our perceptual vision system is able to perceive the objects in the world as stable, although the receptive fields, which operate on the set of image values over local regions in image space, will then be exposed to input information that may differ significantly between different views of the same object. In this work, we explore the consequences of using covariance properties of the visual receptive fields as a fundamental constraint, to make it possible to compare and relate the receptive field responses from different views, with *a priori* possible unknown geometric image transformations between such views.

of the receptive fields at the earliest levels in the visual processing hierarchy. In a theoretically motivated and axiomatically determined normative theory of visual receptive fields (Lindeberg 2013a, 2021), idealized models for the receptive fields of simple cells in the primary visual cortex (V1) have specifically been derived, that lead to provable covariance properties under spatial affine transformations, and regarding extensions to time-dependent spatio-temporal image data also provable covariance properties under Galilean transformations, to handle the variabilities in the relative motion between the objects in the world and the observer, see Lindeberg (2023, 2024c) for more in-depth treatments regarding the importance of covariance properties for visual receptive fields under geometric image transformations.

From a computational viewpoint, if we regard the earliest layers in the visual perception system as a computational engine, that infers successively more complex cues about the structure of the environment from the image measurements that reach the retina, then covariance properties of visual receptive fields do from a theoretical perspective constitute a highly useful notion. Specifically, if we design a computational algorithm for computing the local surface orientation of a smooth surface patch from binocular cues, then compared to not basing the computations on covariant spatial receptive fields, the use of provably affine-covariant visual receptive fields can improve the accuracy by an order of magnitude in estimates of the local surface orientation (see Tables 1–4 in Lindeberg and Gårding (1997)), by elim-

inating a source of error corresponding to a mismatch between the backprojected receptive fields to the tangent plane of the surface, from the two different perspective views, see Figure 2 for an illustration.

Given these theoretically motivated considerations, which have also been empirically tested in computer vision algorithms, one could then raise the question whether the biological vision systems in higher mammals could be regarded as obeying covariance properties under affine spatial transformations, and thus spanning a variability over the degrees of freedom of 2-D spatial affine transformations.

The subject of this paper is to address this issue, by:

- first theoretically describing the different degrees of freedom in spatial affine transformations, in terms of a canonical parameterization, based on a closed-form factorization of the affine transformation matrix A very closely related to a singular value decomposition,
- relating these degrees of freedom to the degrees of freedom in the parameters of the idealized receptive models of simple cells in the primary visual cortex, in terms of the generalized Gaussian derivative theory for visual receptive fields, and finally
- relating these results to existing evidence regarding variabilities in the shapes of biological receptive fields established from neurophysiological measurements.

Specifically, we will after an initial overview of related work in Section 2, in Section 3 describe a decomposition of 2-D spatial affine image transformations, based on a closed-form decomposition of the affine transformation matrix in a way very closely related to a singular value decomposition, and which reveals the degrees of freedom of 2-D spatial affine image transformations in a very geometric manner.

Then, after reviewing the covariance properties of the affine Gaussian derivative model for visual receptive fields in Section 4, we will in Section 5 explicitly describe the degrees of freedom in the affine Gaussian derivative model for visual receptive fields.

Based on this theoretical basis, we will then in Section 6 relate the degrees of freedom in the affine Gaussian derivative model to the degrees of freedom revealed by our proposed decomposition of 2-D affine transformations, in terms of explicit mappings between the parameters in our decomposition of 2-D spatial affine transformations and the parameters in the affine Gaussian derivative model. These connections will then be used in Section 7 for addressing the question of whether we can regard the receptive fields in the primary visual cortex as being able to span the degrees of freedom of 2-D affine transformations.

Finally, Section 8 gives a summary of the main results, with suggestions to further neurophysiological studies to firmly determine to what extent the presented biological hypotheses hold in the primary visual cortex, and then also for what

species, as well as outlooks concerning further implications of the presented theoretical results.

The presented results are aimed at providing a theoretical understanding of basic covariance properties for the earliest layers of receptive fields in computational vision, as well as for generating hypotheses about the computational functions in the earliest levels of visual processing in biological vision.

2 Relations to previous work

Characterizing the functions of the receptive fields in the early visual pathway in terms of computational models constitutes a main topic in the task of understanding the functionalities in the primary visual cortex.

With regard to the task of characterizing the functionality of simple cells, neurophysiological recordings of receptive field profiles of simple cells in the primary visual cortex have been performed by, among others, DeAngelis *et al.* (1995, 2004), Ringach (2002, 2004), Conway and Livingstone (2006), Johnson *et al.* (2008), Ghodrati *et al.* (2017), Walker *et al.* (2019) and De and Horwitz (2021).

The receptive field shapes of simple cells have, in turn, been modelled mathematically in terms of, most commonly, either Gabor filters by Marcelja (1980), Jones and Palmer (1987a, 1987b), Porat and Zeevi (1988), Ringach (2002, 2004), or Gaussian derivatives by Koenderink and van Doorn (1984, 1987, 1992) Young and his co-workers (1987, 2001, 2001) and Lindeberg (2013a, 2021).

Functional modelling of different processes in biological vision has also specifically been performed in terms of Gaussian derivatives by Lowe (2000), May and Georgeson (2007) Hesse and Georgeson (2005), Georgeson *et al.* (2007), Wallis and Georgeson (2009), Hansen and Neumann (2008), Wang and Spratling (2016) and Pei *et al.* (2016).

With regard to spatial scaling transformations of the image data that is registered by a visual observer, at a higher level of abstraction, evidence for processing over multiple scales, with scale invariance constituting a basic functional property in biological vision, have been presented by Biederman and Cooper (1992), Logothetis *et al.* (1995), Ito *et al.* (1995), Furmanski and Engel (2000), Hung *et al.* (2005), Wiskott (2006), Isik *et al.* (2013), Murty and Arun (2017), Benvenuti *et al.* (2018) and Han *et al.* (2020).

Studies of the geometric relationships between pairwise binocular views have been presented by Koenderink and van Doorn (1976), Jones and Malik (1992), Gårding and Lindeberg (1994), Mitiche and Létang (1998), Aczél *et al.* (1999), Uka and DeAngelis (2002), Hansard and Horaud (2008) and Turski (2016, 2024), and more general studies of the image geometry between multiple views by Hartley and Zisserman (2004) and Faugeras (1993).

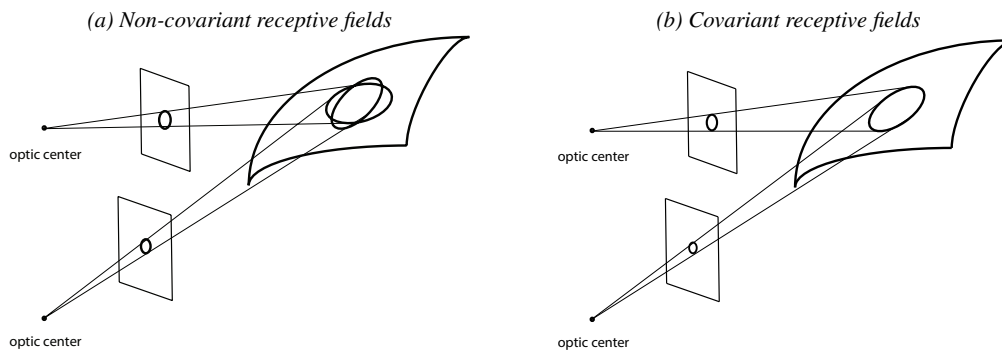


Fig. 2 Geometric illustration of the motivation for the underlying hypothesis concerning affine covariant receptive fields in biological vision. The importance of the notion of covariance for the receptive fields under geometric image transformations originates from the difference in the backprojected receptive fields that will result, if the receptive fields are not covariance. (a) In the left figure, which shows backprojections of non-covariant receptive fields to the tangent plane of a local surface patch, it is clear that largely different support regions in the tangent plane to the surface will affect the receptive field responses for observations of the same surface patch from different viewing directions. (b) In the right figure, which shows backprojections of covariant receptive fields, for which the parameters of the receptive fields have been additionally matched, such that the backprojections of the receptive fields for the two different observations are equal, the contributions from the different image points within the spatial support regions of the visual receptive fields will contribute in a similar manner to the receptive field responses, which implies that the mismatch source of error to cues about properties of the environment will, to first order of approximation, be completely eliminated. (Figures adapted from Lindeberg (2023) with permission (OpenAccess).)

Concerning invariances of image features to geometric image transformations, invariant representations have been modelled in terms of group theory by Poggio and Anselmi (2016). An overview of computational methods to achieve invariance to scaling transformations and locally linearized perspective transformations for monocular cues, as well as locally linearized projections between projective pairwise views, within a larger framework that also involves invariances to Galilean transformations in joint space-time, has been given in (Lindeberg 2013b). Specifically, it is proposed in (Lindeberg 2013a, 2013b, 2021) how covariance properties of the receptive fields in the earliest layers of the visual hierarchy make it possible to compute invariant image features at the higher levels, to, for example, support invariant object recognition.

In view of such a computational view to geometric invariance and covariance properties, one may therefore ask if the receptive fields in the primary visual cortex would be covariant under the basic classes of geometric image transformations, as proposed in (Lindeberg 2023).

The subject of this paper is to address this issue with regard to special case of spatial affine image transformations, and specifically based on a canonical decomposition of such 2-D spatial affine transformations, on a product form of a uniform scaling transformation, pure rotations, a non-uniform scaling transformation, and a normalization of the non-uniform scaling transformation to a preferred symmetry orientation in the image domain.

An earlier study of parameterizations of affine transformations, which we will build upon in this work, was presented in (Lindeberg 1995). In this paper, we extend that parameterization by first of all providing an explicit deriva-

tion in Appendix A.1, which was not presented in the original paper because of space limitations, and then analysing the properties of this decomposition for four basic classes of primitive affine transformations in Appendix A.2. We do additionally give a more general treatment regarding special cases for the parameters in the affine transformation model, which thereby increases the domain of applicability of the proposed parameterization to more general families of affine transformation matrices, that are reasonably near the unit matrix multiplied by a scalar scaling factor.

Then, we will relate the degrees of freedom obtained from this decomposition arising parameterization of 2-D spatial affine transformations to the variabilities in the shapes of the receptive fields in the primary visual cortex.

3 The degrees of freedom in 2-D spatial affine transformations

Let us parameterize the affine transformation matrix \mathcal{A} in the affine transformation (1) as

$$\mathcal{A} = \begin{pmatrix} a_{11} & a_{12} \\ a_{21} & a_{22} \end{pmatrix} \quad (2)$$

and parameterize the image coordinates as $x = (x_1, x_2)^T$ and $x' = (x'_1, x'_2)^T$, where we are here specifically interested in the special case when the affine transformation matrix \mathcal{A} is reasonably close to the unit matrix \mathcal{I} multiplied by some scalar scaling factor.

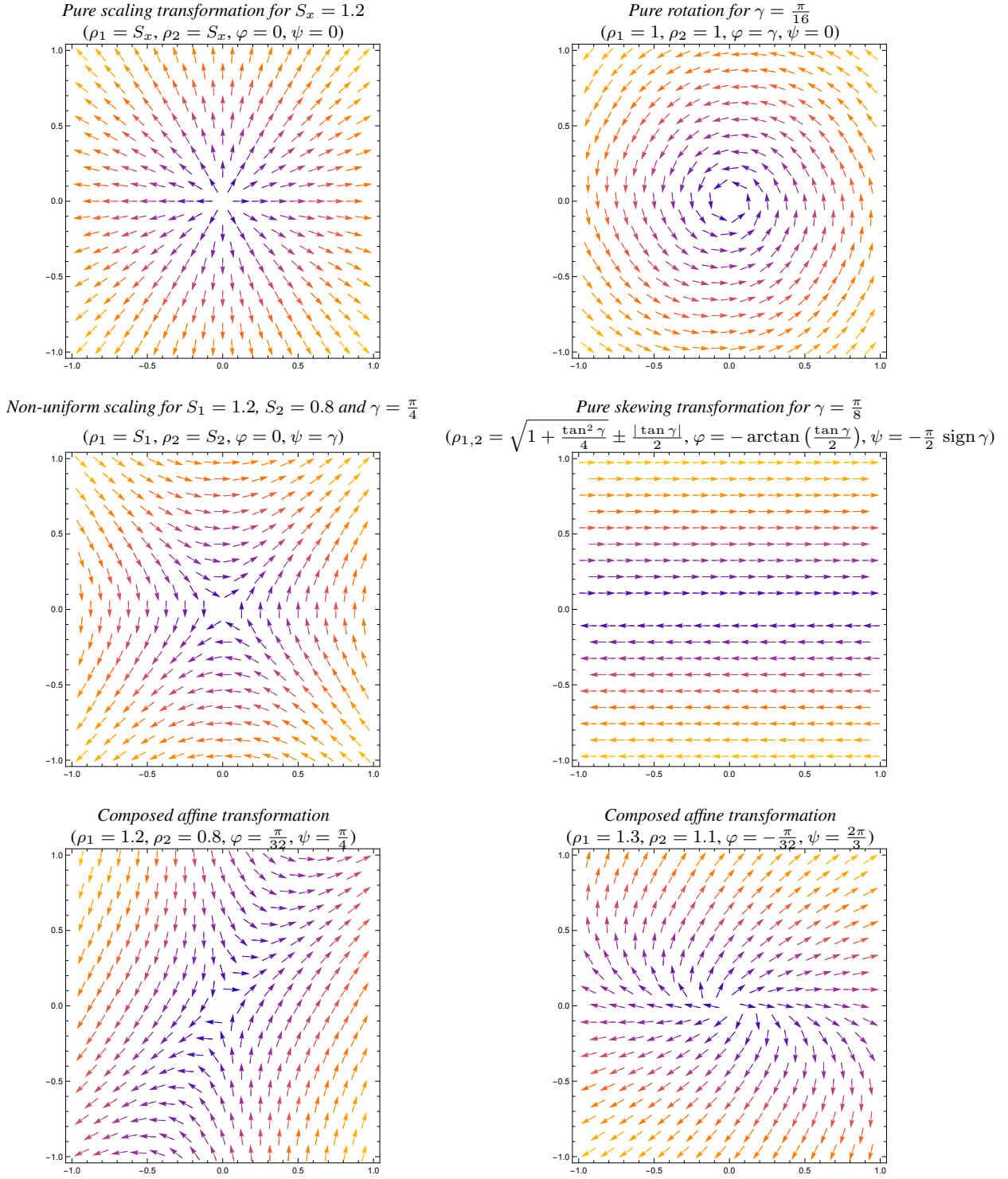


Fig. 3 Visualizations of deformation fields $\Delta x = x' - x = \mathcal{A}x - x = (\mathcal{A} - \mathcal{I})x$ (top and middle rows) for four basic types of primitive affine transformations and (bottom row) two composed affine image transformations, with the directions of the deformation vectors Δx shown as arrows of unit length, and with the magnitude of the deformation coded in colour, with blue corresponding to low magnitudes and yellow to higher magnitudes. For illustration, also the parameters $(\rho_1, \rho_2, \varphi, \psi)$ in the proposed decomposition of the affine transformation matrix according to (18) are also shown, based on the detailed analysis of these four special cases of primitive affine image transformations in Appendix A.2, with specifically the pure scaling transformation matrix according to (102), the pure rotation matrix according to (113), the non-uniform scaling transformation according to (124) and the skewing transformation according to (137). (**Horizontal axes:** spatial coordinate x_1 . **Vertical axes:** spatial coordinate x_2 .)

Following Section 3 in (Lindeberg 1995), let us next define the following descriptors from the elements a_{ij} of \mathcal{A} :

$$T = \frac{a_{11} + a_{22}}{2}, \quad (3)$$

$$A = \frac{a_{21} - a_{12}}{2}, \quad (4)$$

$$C = \frac{a_{11} - a_{22}}{2}, \quad (5)$$

$$S = \frac{a_{12} + a_{21}}{2}. \quad (6)$$

Let us also define the following derived descriptors

$$P = \sqrt{T^2 + A^2}, \quad (7)$$

$$Q = \sqrt{C^2 + S^2}. \quad (8)$$

Then, according to the treatment in Appendix A.1, specifically Equations (88)–(89), it follows that, if we decompose the affine transformation matrix \mathcal{A} into a modified singular value decomposition of the form

$$\mathcal{A} = \mathcal{R}_\alpha \text{diag}(\rho_1, \rho_2) \mathcal{R}_\beta^T, \quad (9)$$

where

$$\mathcal{R}_\alpha = \begin{pmatrix} \cos \alpha & -\sin \alpha \\ \sin \alpha & \cos \alpha \end{pmatrix} \quad (10)$$

and

$$\mathcal{R}_\beta = \begin{pmatrix} \cos \beta & -\sin \beta \\ \sin \beta & \cos \beta \end{pmatrix} \quad (11)$$

are enforced to be pure rotation matrices, then the diagonal entries ρ_1 and ρ_2 in the diagonal matrix $\text{diag}(\rho_1, \rho_2)$ in the decomposition (9) are given by

$$\rho_1 = P + Q, \quad (12)$$

$$\rho_2 = P - Q. \quad (13)$$

Due to our assumption of the affine transformation being reasonably close to the unit matrix \mathcal{I} multiplied by some scalar scaling factor, we will for the purpose of this treatment specifically assume that $\rho_1 > \rho_2 > 0$, such that the decomposition (9) also constitutes a genuine singular value decomposition¹ of the affine transformation matrix \mathcal{A} , with the notable distinction that the matrices \mathcal{R}_α and \mathcal{R}_β are here guaranteed to be actual rotation matrices.

If we furthermore define the following angles

$$\tan \varphi = \frac{A}{T}, \quad (14)$$

$$\tan \psi = \frac{S}{C}, \quad (15)$$

¹ Note that in a general singular value decomposition of an arbitrary affine transformation matrix \mathcal{A} of the form $\mathcal{A} = U \Sigma V^T$, the matrices U and V are only restricted to be unitary matrices, not necessarily rotation matrices.

as well as the corresponding rotation matrices

$$\mathcal{R}_{\frac{\varphi}{2}} = \begin{pmatrix} \cos \frac{\varphi}{2} & -\sin \frac{\varphi}{2} \\ \sin \frac{\varphi}{2} & \cos \frac{\varphi}{2} \end{pmatrix} \quad (16)$$

and

$$\mathcal{R}_{\frac{\psi}{2}} = \begin{pmatrix} \cos \frac{\psi}{2} & -\sin \frac{\psi}{2} \\ \sin \frac{\psi}{2} & \cos \frac{\psi}{2} \end{pmatrix}, \quad (17)$$

then it can be shown (see Appendix A.1 specifically Equations (100) and (101)) that the singular value decomposition of the affine transformation matrix \mathcal{A} , can be factorized on the form

$$\begin{aligned} \mathcal{A} &= \mathcal{R}_{\frac{\psi}{2}} \mathcal{R}_{\frac{\varphi}{2}} \text{diag}(\rho_1, \rho_2) \mathcal{R}_{\frac{\varphi}{2}} \mathcal{R}_{-\frac{\psi}{2}} \\ &= \sqrt{\rho_1 \rho_2} \mathcal{R}_{\frac{\psi}{2}} \mathcal{R}_{\frac{\varphi}{2}} \text{diag}\left(\sqrt{\frac{\rho_1}{\rho_2}}, \sqrt{\frac{\rho_2}{\rho_1}}\right) \mathcal{R}_{\frac{\varphi}{2}} \mathcal{R}_{-\frac{\psi}{2}}, \end{aligned} \quad (18)$$

where

- ρ_1 and ρ_2 are the singular values of \mathcal{A} ,
- the factor

$$S = \sqrt{\rho_1 \rho_2} \quad (19)$$

- corresponds to an overall spatial scaling transformation,
- the diagonal matrix

$$\mathcal{D} = \text{diag}\left(\sqrt{\frac{\rho_1}{\rho_2}}, \sqrt{\frac{\rho_2}{\rho_1}}\right) \quad (20)$$

- describes a non-uniform stretching transformation, corresponding to a relative spatial stretching factor of

$$\lambda = \frac{\rho_1}{\rho_2}, \quad (21)$$

- $\mathcal{R}_{\frac{\psi}{2}}$ and $\mathcal{R}_{\frac{\varphi}{2}}$ are rotation matrices with rotation angles $\frac{\psi}{2}$ and $\frac{\varphi}{2}$, respectively.

In terms of overall effects of the affine transformation, the interpretations of the two rotation angles φ and ψ are then, specifically, that:

- $\varphi = \frac{\varphi}{2} + \frac{\varphi}{2}$ describes the overall total amount of spatial rotation,
- $\frac{\psi}{2}$ represents the orientation of a local symmetry axis for the non-isotropic part of the affine transformation, *e.g.* the pure stretching transformation.

The top and the middle rows in Figure 3 show examples of spatial deformation fields for four basic classes of primitive affine transformations, with the parameters for each one of the different special cases determined according to the analysis of these four special cases in Appendix A.2. The bottom row in Figure 3 does additionally show examples of composed affine deformation fields, as specified from the parameters $(\rho_1, \rho_2, \varphi, \psi)$ in the proposed decomposition of affine transformation matrices according to (18).

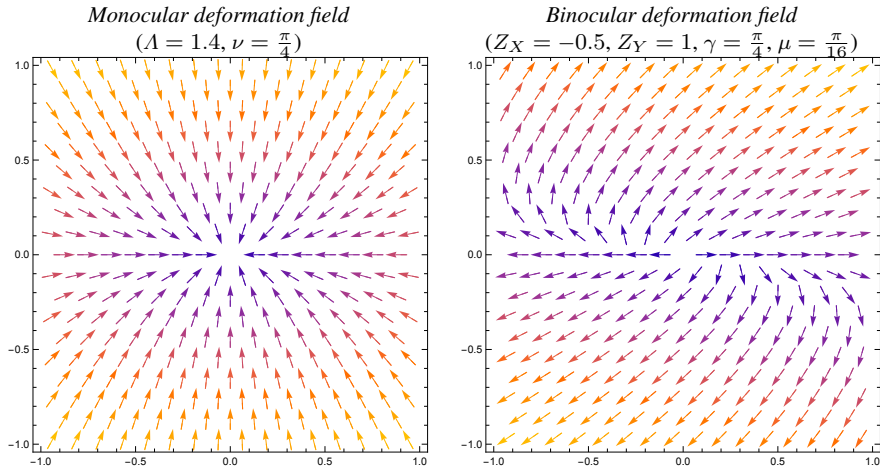


Fig. 4 Visualizations of deformation fields $\Delta x = x' - x = \mathcal{A}x - x = (\mathcal{A} - \mathcal{I})x$ from locally linearized monocular and binocular perspective or projective projection models. **(left)** A monocular deformation field as arising from a locally linearized perspective projection according to (22) of a slanted surface with slant angle ν under variations of the distance Λ between the object and the observer. **(right)** A binocular deformation field as arising from a locally linearized projective mapping between the tangent planes of two smooth surface according to (23), for specific values of the depth gradient $\nabla Z = (Z_X, Z_Y)$, the gaze angle γ between the frontal direction and direction to the fixation point as well as the opening angle 2μ between the viewing directions of the two observers. **(Horizontal axes:** spatial coordinate x_1 . **Vertical axes:** spatial coordinate x_2 .)

3.1 Geometric interpretations of affine image deformations

As previously mentioned, when surface patterns of possibly moving smooth objects in the world are projected to the image plane, by either (i) the perspective mapping to a monocular image, (ii) the projective mapping between two binocular views, or (iii) the temporally integrated optic flow fields obtained by observing moving objects between at adjacent time moments, then the resulting image transformations or deformation fields can to first order of approximation be modelled as local affine transformations.

For this purpose, the decomposition in (18) constitutes a geometrically very natural way to parameterize the degrees of freedom in such local affine transformations of the perspective/projective mappings, and which thus determine the variabilities of the image structures, that a visual system is exposed to, when observing sufficiently smooth surface patterns in the environment from different viewing directions relative to the objects in the environment.

3.1.1 Monocular locally linearized perspective projection

To make such relations more explicit, consider, for example, the monocular perspective projection of a smooth local surface patch onto a spherical camera. Then, in two local coordinate systems, with

- the first local coordinate system being in the tangent plane of the surface patch, with the second local coordi-

nate direction aligned with the tilt² direction of the surface and

- the second local coordinate system being in the tangent plane of the spherical camera, with the second local coordinate direction aligned with the backprojected tilt direction onto the resulting image plane parallel to the tangent plane of the surface,

the first-order locally linearized mapping from the tangent plane of the surface to the tangent plane on the spherical camera is given by (see Gårding and Lindeberg (1996) Equation (28), although here reformulated with somewhat different conventions and notation)

$$\mathcal{A}_{\text{mono}} = \frac{1}{\Lambda} \begin{pmatrix} 1 & 0 \\ 0 & \cos \nu \end{pmatrix}, \quad (22)$$

where

- Λ is the distance between the observed point on the surface of the object and the observer, and
- ν is the slant angle, that is the angle between the surface normal to the surface of the object and the viewing direction.

Figure 4(left) shows a schematic illustration of such a deformation field, as arising from the appearance of deformations of a local surface pattern on a planar surface to the image plane, as we by the local linearization disregard higher-order non-linear components in the perspective mapping.

² The tilt direction is the direction where the depth along a smooth surface varies most strongly.

3.1.2 Binocular locally linearized projective projection

In the binocular case, consider two eyes or cameras that observe a smooth local surface patch from a cyclopean observer. This means that locus of the cyclopean observer is on the midpoint between the two optical centers of the cameras on a circle through the two optical centers and the observed point on the surface, see Figure 1 in Gårding and Lindeberg (1994) for an illustration.

Let 2μ denote the angle between the viewing directions from the two eyes or cameras to the fixation point, and let γ denote the gaze angle between the frontal direction and the direction to the fixation point. Furthermore, let Z_X and Z_Y represent the components of the depth gradient, with Z denoting the depth, and X and Y being the world coordinates parallel to the directions of the image coordinates x_1 and x_2 , respectively. Then, the disparity gradient from the left image to the right image for a calibrated visual observer is given by (see Gårding and Lindeberg (1994) Equation (3))

$$\begin{aligned} \mathcal{A}_{\text{bino}} &= \begin{pmatrix} 1 + h_1 & h_2 \\ v_1 & 1 + v_2 \end{pmatrix} \\ &= \frac{\cos(\gamma - \mu)}{\cos(\gamma + \mu)} \begin{pmatrix} \frac{\cos \mu + Z_X \sin \mu}{\cos \mu - Z_X \sin \mu} & \frac{Z_Y \sin 2\mu}{\cos \mu - Z_X \sin \mu} \\ 0 & 1 \end{pmatrix}, \end{aligned} \quad (23)$$

where $\nabla h = (h_1, h_2)^T$ denotes the horizontal disparity gradient and $\nabla v = (v_1, v_2)^T$ denotes the vertical disparity gradient.

Figure 4(right) shows a schematic example of such a disparity field, as arising from a local linearization between corresponding points under the projective mapping between the two image domain for specific values of the geometric parameters μ , γ and (Z_X, Z_Y) .

4 Covariance properties of affine Gaussian derivative based receptive fields under spatial affine transformations

To characterize the effects that affine image transformations have on receptive field responses, let us next consider receptive fields according to the generalized Gaussian derivative model for visual receptive fields (Lindeberg 2021), and with this regard specifically only consider the effects in relation to the pure spatial and spatio-temporal smoothing transformations applied to static image data or video data, respectively.

4.1 Affine covariance for purely spatial receptive fields

For a purely spatial receptive field applied on pure spatial image data, the influence of a spatial affine transformation

on a receptive field response can be described as the convolution of any input image $f(x)$ with an affine Gaussian kernel $g(x; \Sigma)$ (see Lindeberg (1993) Equation (15.17))

$$L(x; \Sigma) = (g(\cdot; \Sigma) * f(\cdot))(x; \Sigma) \quad (24)$$

where

$$g(x; \Sigma) = \frac{1}{2\pi\sqrt{\det \Sigma}} e^{-x^T \Sigma^{-1} x/2}. \quad (25)$$

Then, it can be shown that, under an affine transformation of the image domain $f'(x') = f(x)$ for $x' = \mathcal{A}x$ according to (1), the corresponding purely spatial scale-space representation according to (24) over the transformed domain

$$L'(x'; \Sigma') = (g(\cdot; \Sigma') * f'(\cdot))(x'; \Sigma') \quad (26)$$

is related to the scale-space representation (24) over the original domain according to

$$L'(x'; \Sigma') = L(x; \Sigma), \quad (27)$$

provided that the spatial covariance matrices Σ' and Σ in the two domains are related according to (see Equations (29) and (30) in Lindeberg and Gårding (1997))

$$\Sigma' = \mathcal{A} \Sigma \mathcal{A}^T. \quad (28)$$

Given these raw purely smoothed components of the receptive field responses, corresponding receptive field responses in terms of spatial derivatives over the two domains, smoothed by affine Gaussian kernels with matching spatial covariance matrices Σ and Σ' , can, in turn, be related according to

$$\nabla_{x'} = \mathcal{A}^{-T} \nabla_x. \quad (29)$$

These relationships, thus, show that, provided that spatial covariance matrices are related in an appropriate way, according to an actual affine image transformation, it is then possible to match the receptive field responses perfectly between the two domains. For such matching to be possible in an actual situation, the actual value of the spatial covariance matrices, and hence the shapes of the corresponding affine Gaussian derivative based receptive fields, must thereby be adapted to the actual affine transformation. Specifically, if the input stimuli involve a variability over a certain subspace or subspace of the degrees of freedom of the affine transformations, then the family of receptive field shapes must also comprise a variability over a that corresponding subspace or subdomain of the parameter space of the affine Gaussian derivative based receptive fields, in order for it to be possible to perfectly match the outputs from the affine Gaussian derivative kernels between the two image domains.

4.2 Affine covariance for joint spatio-temporal receptive fields

A similar analysis can also be performed for joint spatio-temporal receptive fields according to the idealized model (see Lindeberg (2021) Equation (24))

$$T(x, t; \Sigma, \tau, v) = g(x - vt; \Sigma) h(t; \tau) \quad (30)$$

where τ denotes the temporal scale in units of the temporal variance $\tau = \sigma_t^2$ of the temporal smoothing kernel $h(t; \tau)$ and $v = (v_1, v_2)$ denotes an image velocity parameter.

Given two video sequences $f(x, t)$ and $f'(x', t')$, that are related according to a pure spatial affine transformation

$$x' = \mathcal{A}x, \quad \text{and} \quad t' = t, \quad (31)$$

let

$$\begin{aligned} L(x, t; \Sigma, \tau, v) &= \\ &= (T(\cdot, \cdot; \Sigma, \tau, v) * f(\cdot, \cdot))(x, t; \Sigma, \tau, v), \end{aligned} \quad (32)$$

$$\begin{aligned} L'(x', t'; \Sigma', \tau', v') &= \\ &= (T(\cdot, \cdot; \Sigma', \tau', v') * f(\cdot, \cdot))(x', t'; \Sigma', \tau', v'), \end{aligned} \quad (33)$$

denote the spatio-temporal smoothed scale-space representations in the two domains. Then, these joint spatio-temporal scale-space representations are related according to (see Lindeberg (2023) Equation (54))

$$L'(x', t'; \Sigma', \tau', v') = L(x, t; \Sigma, \tau, v), \quad (34)$$

provided that the spatial covariance matrices Σ and Σ' are related according to

$$\Sigma' = \mathcal{A} \Sigma \mathcal{A}^T, \quad (35)$$

as well as provided that the other receptive field parameters are equal, that is $\tau' = \tau$ and $v' = v$. Thus, this result shows that also joint spatio-temporal receptive field responses can be made to perfectly match each other under spatial affine transformations, provided that the spatial shapes of the joint spatio-temporal receptive fields are appropriately adapted with respect to the actual spatial affine transformation.

5 Degrees of freedom in the affine Gaussian derivative model for visual receptive fields

The spatial covariance matrix

$$\Sigma = \begin{pmatrix} C_{11} & C_{12} \\ C_{12} & C_{22} \end{pmatrix} \quad (36)$$

in the affine Gaussian derivative model for visual receptive fields can be parameterized on the form

$$C_{11} = \sigma_1^2 \cos^2 \varphi + \sigma_2^2 \sin^2 \varphi, \quad (37)$$

$$C_{12} = (\sigma_1^2 - \sigma_2^2) \cos \varphi \sin \varphi, \quad (38)$$

$$C_{22} = \sigma_1^2 \sin^2 \varphi + \sigma_2^2 \cos^2 \varphi, \quad (39)$$

where $\lambda_1 = \sigma_1^2$ and $\lambda_2 = \sigma_2^2$ constitute the eigenvalues of Σ . Under variabilities of the spatial scale parameters $\sigma_1 > 0$ and $\sigma_2 > 0$, and the spatial orientation φ , these variabilities span the variability of the shapes of the receptive fields in the receptive field model.

In relation to overall shape properties of the receptive fields, the degrees of freedom in this parameterization have the following interpretation:

- the product

$$\bar{\sigma} = \sqrt{\sigma_1 \sigma_2} \quad (40)$$

- describes the overall *spatial size* of the receptive field,
- the ratio

$$\epsilon = \frac{\sigma_2}{\sigma_1} \quad (41)$$

- describes the eccentricity or the *degree of elongation* of the receptive field, in the sense that deviations in this ratio from the rotationally symmetric special case when $\epsilon = 1$ correspond to more elongated or anisotropic receptive fields, and
- the angle φ in (37)–(39) represents the *spatial orientation* of the receptive field.

Figures 5–7 show illustrations of these variabilities for purely spatial receptive fields, in terms of first- and second-order directional derivatives of affine Gaussian kernels, according to the following idealized models for the receptive fields of simple cells in the primary visual cortex (based on Equation (31) in Lindeberg (2021)):

$$T_{\text{simple}}(x_1, x_2; \sigma_1, \sigma_2, \varphi, m) = \sigma_1^m \partial_\varphi^m g(x_1, x_2; \Sigma), \quad (42)$$

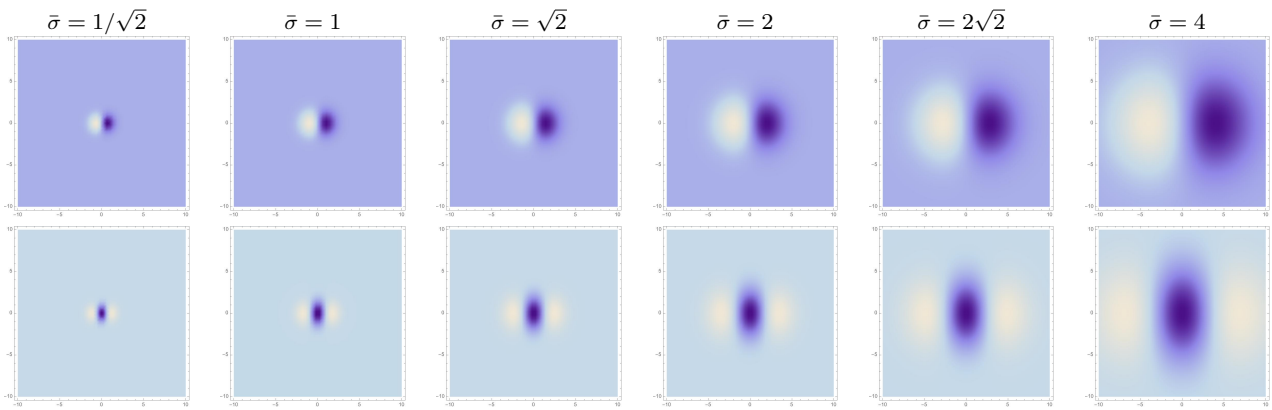


Fig. 5 Variability in the size of affine Gaussian derivative receptive fields (for $\sigma_1 = \sigma_2$ and image orientation $\varphi = 0$), with the overall size $\bar{\sigma} = \sqrt{\sigma_1\sigma_2}$ increasing from $1/\sqrt{2}$ to 4 according to a logarithmic distribution, from left to right. (top row) First-order directional derivatives of affine Gaussian kernels according to (43). (bottom row) Second-order directional derivatives of affine Gaussian kernels according to (44). (**Horizontal axes:** image coordinate $x_1 \in [-10, 10]$. **Vertical axes:** image coordinate $x_2 \in [-10, 10]$.)

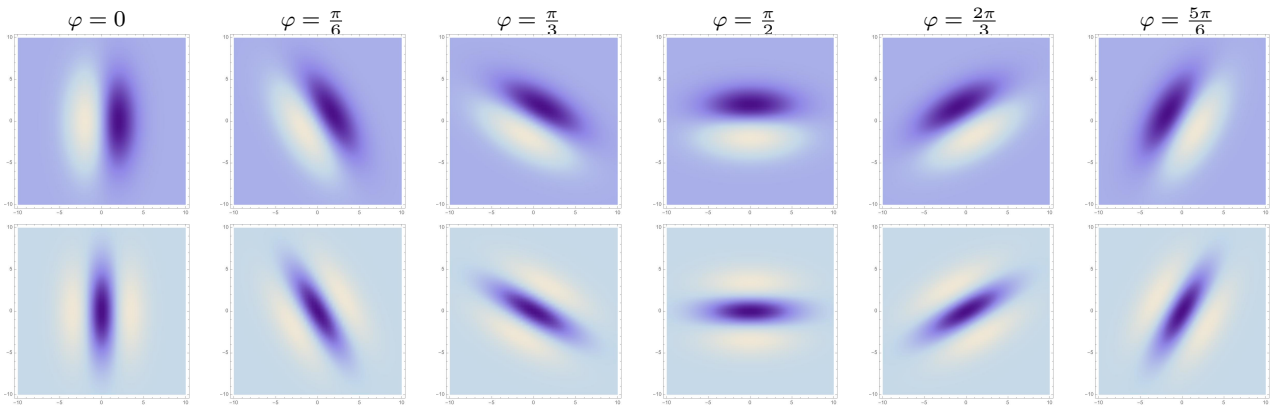


Fig. 6 Variability in the orientation of affine Gaussian derivative receptive fields (for $\sigma_1 = 2$ and $\sigma_2 = 4$), with the orientation angle φ increasing from left to right. (top row) First-order directional derivatives of affine Gaussian kernels according to (43). (bottom row) Second-order directional derivatives of affine Gaussian kernels according to (44). (**Horizontal axes:** image coordinate $x_1 \in [-10, 10]$. **Vertical axes:** image coordinate $x_2 \in [-10, 10]$.)

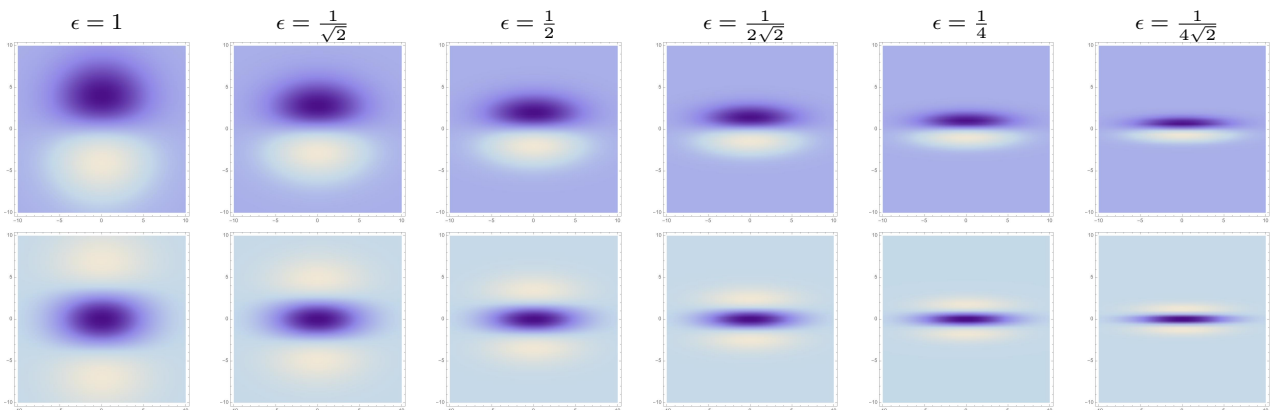


Fig. 7 Variability in the eccentricity of affine Gaussian derivative receptive fields (for image orientation $\varphi = \frac{\pi}{2}$), with the eccentricity $\epsilon = \sigma_1/\sigma_2$ decreasing from 1 to according to a logarithmic distribution, from left to right, with σ_2 kept constant. (top row) First-order directional derivatives of affine Gaussian kernels according to (43). (bottom row) Second-order directional derivatives of affine Gaussian kernels according to (44). (**Horizontal axes:** image coordinate $x_1 \in [-10, 10]$. **Vertical axes:** image coordinate $x_2 \in [-10, 10]$.)

which for first and second orders of spatial differentiation m assume the following explicit forms

$$\begin{aligned} T_{\text{simple}}(x_1, x_2; \sigma_1, \sigma_2, \varphi, 1) &= \\ &= \sigma_1 (\cos(\varphi) \partial_{x_1} + \sin(\varphi) \partial_{x_2}) g(x_1, x_2; \Sigma) \\ &= -\frac{(x_1 \cos(\varphi) + x_2 \sin(\varphi))}{2\pi \sigma_1^2 \sigma_2} \times \\ &e^{-\frac{(\sigma_1^2 + \sigma_2^2)(x_1^2 + x_2^2) - (\sigma_1 - \sigma_2)(\sigma_1 + \sigma_2)(2x_1 x_2 \sin(2\varphi) + \cos(2\varphi)(x_1 - x_2)(x_1 + x_2))}{4\sigma_1^2 \sigma_2^2}} \end{aligned} \quad (43)$$

$$\begin{aligned} T_{\text{simple}}(x_1, x_2; \sigma_1, \sigma_2, \varphi, 2) &= \\ &= \sigma_1^2 (\cos^2(\varphi) \partial_{x_1 x_1} + 2 \cos(\varphi) \sin(\varphi) \partial_{x_1 x_2} + \sin^2(\varphi) \partial_{x_2 x_2}) \\ &\quad g(x_1, x_2; \Sigma) \\ &= \frac{(\cos(2\varphi)(x_1^2 - x_2^2) + 2x_1 x_2 \sin(2\varphi) - 2\sigma_1^2 + x_1^2 + x_2^2)}{4\pi \sigma_1^3 \sigma_2} \times \\ &e^{-\frac{(\sigma_1^2 + \sigma_2^2)(x_1^2 + x_2^2) - (\sigma_1 - \sigma_2)(\sigma_1 + \sigma_2)(2x_1 x_2 \sin(2\varphi) + \cos(2\varphi)(x_1 - x_2)(x_1 + x_2))}{4\sigma_1^2 \sigma_2^2}} \end{aligned} \quad (44)$$

Figures 5–7 illustrate the basic variabilities of the shapes of the receptive fields arising in this way according to the affine Gaussian derivative model. A main question addressed in this paper concerns what variabilities in receptive field shapes may be spanned in the primary visual cortex.

6 Relationships between the variabilities in affine image transformations and the variabilities in affine Gaussian receptive fields

From a comparison between the degrees of freedom in 2-D spatial affine transformations according to Section 3 with the degrees of freedom in the shapes of the affine Gaussian receptive fields in Section 5, it does specifically hold that:

- variabilities in the *size* of the overall size receptive field, as represented by the product

$$\bar{\sigma} = \sqrt{\sigma_1 \sigma_2} \quad (45)$$

in (40), span the variability over the overall *spatial scaling factor*

$$S = \sqrt{\rho_1 \rho_2} \quad (46)$$

according to (19) in the affine image transformations,

- variabilities in the *eccentricity* of the receptive field, as can be described by the ratio

$$\epsilon = \frac{\sigma_2}{\sigma_1} \quad (47)$$

in (41), do, for a fixed value of the image orientation angle φ of the affine Gaussian receptive fields, span the variability in the *ratio between the singular values*

$$\lambda = \frac{\rho_1}{\rho_2} \quad (48)$$

of the affine transformation, which, in turn, represents the essential variability in the amount of non-uniform spatial stretching in the pure stretching transformation \mathcal{D} according to (20) in the affine image transformations, – variabilities in the *orientation angle*

$$\varphi \quad (49)$$

of the affine Gaussian receptive fields according to (37)–(39) span the variability in the amount of *overall rotation* φ of the total rotation component

$$\mathcal{R}_\varphi = \mathcal{R}_{\frac{\varphi}{2}} \mathcal{R}_{\frac{\varphi}{2}} \quad (50)$$

according to (18) in the affine image transformations.

In these respects, there is a one-to-one mapping between three of the degrees of freedom of 2-D spatial affine transformations and the three degrees of freedom in the regular formulation of idealized receptive field models in terms of the regular formulation of directional derivatives of affine Gaussian kernels.

Specifically, if the image data in an imaging situation would be subject to these degrees of freedom in 2-D spatial affine transformations, we can then let the affine Gaussian derivative kernels exhibit corresponding variabilities in the shapes of their receptive fields, to be able to match the receptive field responses between the image domains before vs. after the affine image deformation.

6.1 Restricted 3-D variability of regular affine Gaussian derivative kernels

Because the variability of the shapes of affine Gaussian receptive fields in three-dimensional, while the variability of the affine image transformations is four-dimensional, the variability of the shapes of the receptive fields according to the affine Gaussian derivative model used for formulating the explicit expressions for the idealized models for the receptive fields of simple cells according to Equations (43) and (44), with the directions for which the directional derivatives of the affine Gaussian kernels are computed in directions parallel with the eigendirections of the affine Gaussian kernels, cannot, in its original formulation, span the full variability of the affine group.

6.2 Possible extensions to a 4-D variability to enable matching of affine Gaussian derivative responses

An operational explanation why affine covariance cannot be achieved for the regular affine Gaussian derivative kernels, with the orientation for computing the directional derivative of that regular affine Gaussian derivative kernel being

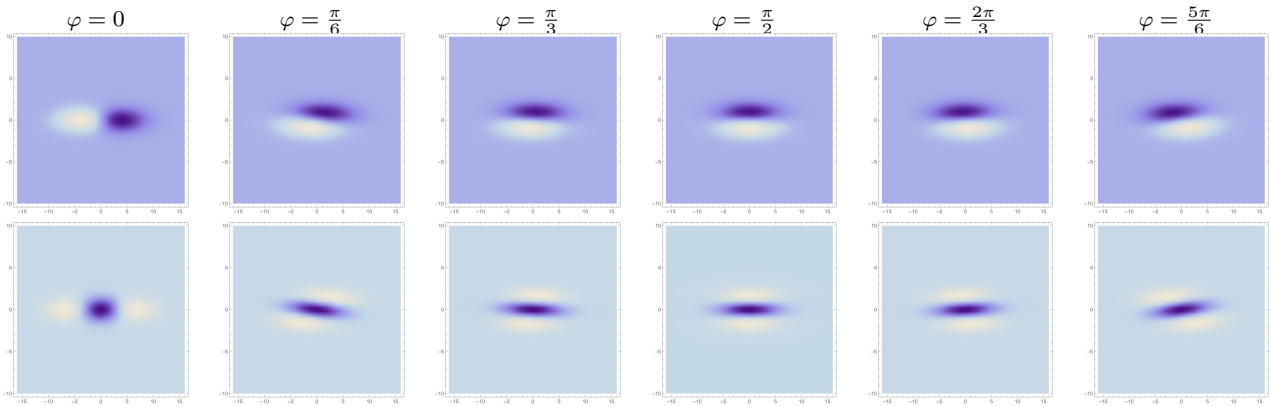


Fig. 8 Variability in the orientation of directional derivatives of affine Gaussian derivative receptive fields (for $\sigma_1 = 4$ and $\sigma_2 = 1$), with the orientation angle φ increasing from left to right. (top row) First-order directional derivatives of affine Gaussian kernels. (bottom row) Second-order directional derivatives of affine Gaussian kernels. (**Horizontal axes:** image coordinate $x_1 \in [-10, 10]$. **Vertical axes:** image coordinate $x_2 \in [-10, 10]$.)

required to be aligned with a principal direction of the covariance matrix of the affine Gaussian kernel, is that if the affine image transformation comprises a non-uniform scaling transformation in a direction that not coincides with the principal directions of the spatial covariance matrix in the affine Gaussian smoothing kernel, then the transformed receptive field of a regular affine Gaussian derivative kernel, will be no longer within the definition of such a regular affine Gaussian directional derivative kernel.

Instead, to enable full affine covariance, the image orientation of the directional derivative operator in the transformed affine Gaussian derivative kernel must be allowed to be different from the restriction of the image direction for the directional derivative being aligned to either of the principal directions of the affine Gaussian smoothing kernel.

6.2.1 Alternative 1: Explicit expansion of the directions of directional derivatives of affine Gaussian kernels

The variability of the receptive fields of receptive fields according to the affine Gaussian derivative model for visual receptive fields can, however, be extended, by allowing the orientation angle for which the directional derivatives in the direction φ of the affine Gaussian derivative kernels according to (42)

$$T_{\text{simple}}(x_1, x_2; \sigma_1, \sigma_2, \varphi, m) = \sigma_1^m \partial_{\varphi}^m g(x_1, x_2; \Sigma), \quad (51)$$

are computed, to instead be allowed to be computed in directions in the spatial domain that do not necessarily have to be aligned with either of the eigenvectors of the spatial covariance matrix Σ , see Figure 8 for examples of such receptive fields for fixed values of the spatial scale parameters σ_1 and σ_2 . Then, such extended models for the spatial receptive fields, which will span a four-dimensionality, will allow for expanded covariance properties over the

full group of non-singular spatial affine transformations, according to the treatment in (Lindeberg 2024c Section 3.5).

6.2.2 Alternative 2: Expanded matching to linear combinations of affine Gaussian directional derivatives as opposed to restricted matching to just plain receptive field responses

Concerning the above possible extension, it should, however, be noted that due to the definition of directional derivatives, the directional derivative of a 2-D affine Gaussian kernel can be parameterized to the form

$$\begin{aligned} T_{\varphi^{m_1} \perp \varphi^{m_2, \text{norm}}}(x_1, x_2; \sigma_1, \sigma_2, \varphi, m) \\ &= \partial_{\varphi, \text{norm}}^{m_1} \partial_{\perp \varphi, \text{norm}}^{m_2} g(x_1, x_2; \Sigma) \\ &= \sigma_1^{m_1} (\cos \varphi \partial_{x_1} + \sin \varphi \partial_{x_2})^{m_1} \\ &\quad \sigma_2^{m_2} (-\sin \varphi \partial_{x_1} + \cos \varphi \partial_{x_2})^{m_2} g(x_1, x_2; \Sigma), \quad (52) \end{aligned}$$

where $\perp \varphi$ denotes the orthogonal direction to φ .

Therefore, given a fixed value of the spatial covariance matrix Σ , it is sufficient to compute the directional derivatives in $m + 1$ sufficiently different directions, in order to then be able to span the space for computing the directional derivative of order $m = m_1 + m_2$ in any other direction, according to

$$\begin{aligned} T_{\varphi^m}(x_1, x_2; \sigma_1, \sigma_2, \varphi, m) &= \\ &= \sum_{k=1}^M p_k T_{\varphi_k^m}(x_1, x_2; \sigma_1, \sigma_2, \varphi_k, m), \quad (53) \end{aligned}$$

for some $M \geq m + 1$ and some constants p_k . For this purpose, the actual values for the parameters p_k can, in turn, be determined by setting up and solving a linear system of equations relations, based on relationships of the form (52),

mapped down to relationships in terms of the partial derivatives $\partial_{x_1^i x_2^{m-i}} g(x_1, x_2; \Sigma)$ as the underlying basis for these relationships for all $j \in [0, m]$.

Thus, from a computational viewpoint, it is not necessary to fully span the variability of this fourth dimension, while nevertheless being able to match the receptive field responses between the two domains, if we would simultaneously expand the matching process to not just match plain receptive field responses between the two domains, but instead allow for matching of the receptive field response from the first image domain to a linear combination of receptive field responses over the second image domain of the form

$$\begin{aligned} T_{\varphi^m}(x_1, x_2; \sigma_1, \sigma_2, \varphi, m) * f(x_1, x_2) = \\ = \sum_{k=1}^M q_k T_{\varphi_k^m}(x'_1, x'_2; \sigma'_1, \sigma'_2, \varphi'_k, m) * f'(x'_1, x'_2) \end{aligned} \quad (54)$$

for some constants q_k chosen specific to the relationships between the orientation φ in the first domain and the selection of sampled orientations φ' in the second domain, as well as also depending on the degrees of freedom of the affine transformation matrix \mathcal{A} .

Note, however, that for such a computational structure to work, for directional derivatives of higher orders $m \geq 2$, it is not sufficient to use the directional derivatives along the eigendirections of the spatial covariance matrix Σ as the basis. Instead, for directional derivative orders $m \geq 2$, directional derivatives would also have to be computed in directions that are significantly different from the eigendirections of the spatial covariance matrix Σ . Furthermore, that number of additional required complementary directions for directional derivative computations would be required to increase with the order m of spatial differentiation.

7 Which degrees of freedom of 2-D spatial affine transformations are spanned by the receptive fields in the primary visual cortex?

Given (i) these theoretical results, and given that (ii) the biological receptive fields corresponding to simple cells in the primary visual cortex, as measured by (1995, 2004), Conway and Livingstone (2006) and Johnson *et al.* (2008), can be qualitatively rather well modelled with spatial components in terms of affine Gaussian derivatives according to the axiomatically derived normative theory for visual receptive fields in Lindeberg (2013a, 2021), one may ask if biological vision has also developed corresponding variabilities in receptive field shapes as would be predicted from the presented theory. Specifically, one may ask if the shapes of the simple cells in the primary visual cortex would have the ability to span the variabilities corresponding to 2-D spatial affine transformations.

As previously stated, a highly useful property of affine covariant receptive fields in computer vision is that they allow for substantially more accurate inference of shape from monocular or binocular cues as opposed to non-covariant receptive fields, see Tables 1–4 in Lindeberg and Gårding (1997) for numerical results of computing estimates of local surface orientation with using a procedure that successively updates the shapes of the receptive fields to previous orientation estimates, which then leads to substantially lower errors in the surface orientation estimates after just a few iterations.

As previously argued in Lindeberg (2021) Section 6, it could specifically also constitute an evolutionary advantage for higher species, that rely on visual information as a critical source of information about the environment, to adapt their vision systems to the geometrical properties of the image formation process. Specifically, an expansion of the image data over the degrees of freedom over the parameters of natural image transformations would be consistent with the substantial number of receptive fields in the early visual pathway, with

- about 100 M photoreceptors and 1 M output channels in and from the retina to the lateral geniculate nucleus (LGN),
- about 1 M neurons in the LGN and about 1 M output channels to the primary visual cortex (V1), then
- with about 190 M neurons in V1 and about 37 M output channels from V1,

see Figure 3 in DiCarlo *et al.* (2012).

The subject of this section is to use the theoretical treatment developed in the previous sections to consider whether we could from such a view regard the receptive fields in the primary visual cortex to exhibit variabilities in their shapes, that could be interpreted as if the receptive fields would have the ability to span the variabilities generated by the family of 2-D spatial affine transformations.

7.1 Variability under uniform scaling transformations

The issue of a possible variability of the receptive fields with respect spatial scaling transformations is special, in the sense that, according to the theory for affine Gaussian receptive fields, the receptive fields at coarser levels of scale can, in principle, be computed from the receptive fields at finer levels of scales.

Due to the semi-group property of the affine Gaussian kernel (see Lindeberg (1993) Equation (15.35))

$$g(\cdot; \Sigma_1) * g(\cdot; \Sigma_2) = g(\cdot; \Sigma_1 + \Sigma_2), \quad (55)$$

it follows that by combining *e.g.* the output from the receptive fields corresponding to first-order spatial derivatives

$$(\nabla_x L)(\cdot; \Sigma_1) = (\nabla_x g)(\cdot; \Sigma_1) * f(\cdot), \quad (56)$$

where $\nabla_x = (\partial_{x_1}, \partial_{x_2})^T$, over different positions in image space, we can from the output of such a first layer of visual processing, compute the responses of the first-order derivatives at any coarser level of scale

$$(\nabla_x L)(\cdot; \Sigma_2) = (\nabla_x g(\cdot; \Sigma_2)) * f(\cdot), \quad (57)$$

by combining the outputs from the first layer with suitable weights, such that the resulting computations implement a convolution operation of the following form

$$(\nabla_x L)(\cdot; \Sigma_2) = g(\cdot; \Sigma_2 - \Sigma_1) * (\nabla_x L)(\cdot; \Sigma_1), \quad (58)$$

provided that the difference between the spatial covariance matrices

$$\Delta\Sigma = \Sigma_2 - \Sigma_1 \quad (59)$$

is a symmetric positive definite matrix.

In fact, concerning receptive fields in the retina, an interpretation of results concerning measurements of receptive fields at different distances from the center of the fovea, in combination with a theoretically principled model of a foveal scale space, with the complementary essential requirement of a limited processing capacity in terms of a finite number of neurons, are consistent with the interpretation that the minimum size of the receptive fields, at any distance from the center of the fovea, should increase linearly with the distance from the center of the fovea (see Lindeberg (2013a) Section 7).

Thus, irrespective of whether the primary visual cortex would perform an explicit expansion over multiple receptive field sizes over some scale range or not, one could, because of the cascade smoothing property of spatial Gaussian derivative operators, also conceive a possible design strategy for a vision system to only implement a first layer of visual receptive fields at a finest level of scale, and then computing the representations at coarser scale in an implicit manner, from the finer-scale receptive field responses.

Explicit suggestions for neurophysiological experiments to map the possible variability of receptive field shapes over multiple sizes in the image domain are given in Section 3.2.2 in Lindeberg (2023).

7.2 Variability under rotations in the image plane

From the structure of the orientation maps around pinwheels, as pioneered by Bonhoeffer and Grinvald (1991) and Blasdel (1992) (see Figure 9), we can from the above theoretical treatment interpret these results as the receptive fields in the visual cortex could be regarded as spanning a variability over the pure image rotation component φ in (18) in the affine group.

Furthermore, using a stimulus manifold analysis, Beshkov and Einevoll (2023) show that rotating stimuli in the image

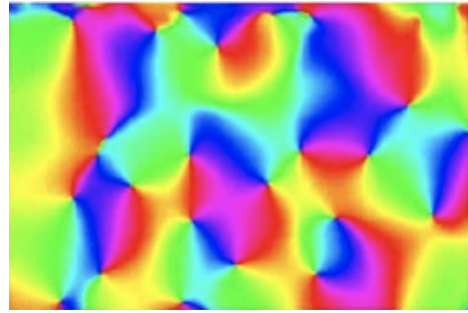


Fig. 9 Orientation map in the primary visual cortex of cat, as recorded by Koch *et al.* (2016) (OpenAccess), and demonstrating that the visual cortex performs an explicit expansion of the receptive field shapes over spatial image orientations, as would be the result of combining the notion of covariance over the subgroup of pure image rotations, and corresponding to a variability over the orientation parameter φ in the proposed decomposition (18) of 2-D spatial affine transformations.

domain leads to the generation of circles in the primary visual cortex, also in very good agreement with the assumption of a covariance property in the primary visual cortex over the degree of freedom in affine image transformations corresponding to pure rotations in the image domain.

7.3 Variability under non-uniform scaling transformations?

In Lindeberg (2024a), an in-depth treatment is given concerning whether the receptive fields in the primary visual cortex could be regarded as spanning a variability over the degree of elongation of the receptive fields.

Based on the relationships between the degrees of freedom in 2-D spatial affine transformations and the degrees of freedom in the affine Gaussian derivative model established in Section 6, the possible existence of such a variability, for the receptive fields in the primary visual cortex of higher mammals with a pinwheel structure, would then correspond to the family of the receptive fields spanning an expansion over the non-isotropic scaling component $\mathcal{D} = \text{diag}(\sqrt{\frac{\rho_1}{\rho_2}}, \sqrt{\frac{\rho_2}{\rho_1}})$ in (18) of the affine group, that is over the parameter $\lambda = \rho_1/\rho_2$ according to (48) in the proposed decomposition of 2-D spatial affine transformations.

Unfortunately, there does, however, not appear to exist any sufficiently extensive direct measurements of the eccentricity or the degree of elongation for sufficiently large populations of visual neurons to firmly answer this question. In Lindeberg (2024a), we have therefore taken an alternative indirect approach to this topic, by making use of existing biological measurements of orientation selectivity by Nauhaus *et al.* (2008), who have reported that there is a substantial variability in the orientation selectivity of the visual receptive fields in relation to the pinwheel structure for monkeys and cats. Goris *et al.* (2015) have also accumu-

lated histograms of the resultant of the orientation selectivity curves for simple cells and complex cells.

In Lindeberg (2024b), we have performed an in-depth theoretical analysis of the orientation selectivity properties of idealized models of the receptive fields of simple and complex cells in terms of affine Gaussian derivatives, and shown that there is a direct connection between the orientation selectivity and the degree of elongation of the receptive fields according to the affine Gaussian derivative model. In Lindeberg (2024a) we have furthermore computed closed-form expressions for the resultant of the orientation selectivity curves for the idealized model for visual receptive fields based on affine Gaussian derivatives, and demonstrated that such a closed-form theoretical analysis leads to predictions about histograms of the resultants of orientation selectivity curves for the corresponding idealized models of simple cells that are in very good qualitative agreement with experimentally obtained histograms from biological neurons by Goris *et al.* (2015).

If we could assume that the idealized generalized affine Gaussian derivative model would constitute a sufficiently accurate model for the receptive fields of the visual neurons in the primary visual cortex, then we would be able to logically infer that there ought to be a variability over the degree of elongation of the receptive fields in the biological neurons. Such logically based modelling arguments are, however, not necessarily guaranteed to hold, if there would be other factors, not incorporated into the idealized models of the receptive fields, that could also affect the orientation selectivity of the receptive fields.

To more firmly determine whether the hypothesis about an expansion over the degree of elongation of the receptive fields would hold for actual biological neurons, a set of more explicit biological hypotheses, with suggestions for complementary quantitative measurements, have therefore been formulated in Sections 3.2–3.3 in Lindeberg (2024a) to answer this question, and if the working hypothesis would hold, then also characterize how such a possible variability in the degree of elongation of the receptive fields would relate to the pinwheel structures in the orientation maps of the primary visual cortex.

7.4 Possible variability over a fourth degree of freedom?

Concerning a possible additional variability over the remaining fourth degree of freedom of affine transformations, we did in Section 6.2 discuss two ways by which affine Gaussian derivative model with a genuine 3-D variability could be extended to four degrees of freedom.

Notably, in relation to his Gabor modelling of visual receptive fields, Ringach *et al.* (2002) found that for a majority of the receptive fields that he modelled in that study, he

did not find it necessary to add a parameter to vary the orientation of the non-isotropic Gaussian kernel in relation to the orientation of the cosine wave; such a parameter “helped only in a small number of cases” (see Ringach *et al.* 2002, page 457).

Given that a few receptive fields, hence, obviously have been recorded, for which a Gabor-based modelling of receptive fields would be helped by having the principal axes of an affine Gaussian kernel being not oriented in a similar orientation as the principal axis of the cosine function in the Gabor model, one may ask, if when instead modelling those receptive fields by directional derivative of affine Gaussian kernels, such a modelling would be helped by not having the orientation of the directional derivative operator in the affine Gaussian derivative model being aligned with a principal direction of the affine Gaussian kernel used in that affine Gaussian derivative model.

Given this observation, one may then raise the question of whether it would be possible to accumulate support from neurophysiological experiments for such a variability, which would then constitute support for an expansion of the receptive field shapes over this remaining fourth degree of freedom.

8 Summary and discussion

In this paper, we have, after describing contextual relations to previous work in Section 2, first in Section 3 performed an in-depth characterization of the degrees of freedom in 2-D spatial affine transformations, based on a decomposition of the affine transformation matrix to a product form very closely related to a singular value decomposition, although on closed form, and with the pre-multiplication and post-multiplication matrices V and U in a regular singular value decomposition here required to be pure rotation matrices.

For our target application, where we consider affine transformation matrices reasonably close to a unit matrix multiplied by a positive scaling factor, such a product form does indeed guarantee positive diagonal entries in the diagonal matrix of the proposed matrix decomposition. In Appendix A.1, we have specifically shown how the parameters $(\rho_1, \rho_2, \varphi, \psi)$ of the proposed matrix decomposition (18) can be determined from the parameters a_{ij} of the affine transformation matrix \mathcal{A} , which in these ways extend the earlier treatment of this concept in (Lindeberg 1995).

Then, we have, after an overview of the covariance properties of the affine Gaussian derivative model in Section 4, in Section 5 analyzed the degrees of freedom in the affine Gaussian derivative model, to in Section 6 relate the degrees of freedom of the affine Gaussian derivative model to the degrees of freedom in 2-D spatial affine transformations:

- For the uniform spatial scaling factor $S = \sqrt{\rho_1 \rho_2}$ in a spatial affine transformation decomposed according to (19), there is a direct mapping to the the square root of the product of the standard deviations $\bar{\sigma} = \sqrt{\sigma_1 \sigma_2}$ according to (45) of the Gaussian kernel in the principal directions of the spatial covariance matrix Σ .
- For the ratio between the singular values $\lambda = \rho_1/\rho_2$ in the affine decomposition according to (48), there is a direct (inverse) relationship to the eccentricity $\epsilon = \sigma_2/\sigma_1$ according to (47) in the receptive field model based on affine Gaussian derivatives.
- For the total amount of rotation $\mathcal{R}_\varphi = \mathcal{R}_{\frac{\varphi}{2}} \mathcal{R}_{\frac{\varphi}{2}}$ according to (50) in the proposed matrix decomposition (18), there is a direct mapping to variabilities in the orientation φ of the affine Gaussian receptive fields according to (42), provided that the spatial covariance matrix covaries with the angle φ according to (37)–(39).

Due to the fact that the original formulation of idealized models of simple cells $T_{\text{simple}}(x_1, x_2; \sigma_1, \sigma_2, \varphi, m)$ according to the most strict formulation according to (42), with the directional derivative operator parallel to either of the eigendirections of the spatial covariance matrix Σ , only represents a three-dimensional variability, while the variability of affine transformation matrices \mathcal{A} is four-dimensional, the restriction of idealized simple cells to the form (42) cannot span the full variability of 2-D spatial affine transformations.

To enable matching of receptive field responses under the full variability of 4-D spatial transformations, we have therefore in Section 6.2 considered two types of extensions of the original model, to enable perfect matching of receptive field responses under general 2-D spatial affine transformations:

- either by extending the variability of the directions of the directional derivatives to a full variability over image orientations in relation to the eigendirections of the spatial covariance matrix Σ , which, however, then would lead to a highly redundant representation, since the directional derivatives in different directions are related in terms of linear combinations,
- or indirectly representing just the subspace of such a full variability with a set of at least $m + 1$ sampled and sufficiently different image orientations φ_k in relation to the eigendirections of the spatial covariance matrix, and then performing the matching to linear combinations of receptive field responses within that subspace, as opposed to perfect pairwise matching of receptive field responses between the two image domains that are related by a 2-D spatial affine transformations.

In these ways, we have described how the idealized affine Gaussian derivative model allows for explicit matching of first of all spatial receptive field responses under general 2-D spatial affine transformations, based on the covariance prop-

erties of the spatial affine Gaussian derivative model according to the treatment in Section 4.1. With extension of the spatial affine covariance properties to spatio-temporal affine covariance according to Section 4.2, the proposed model does additionally allow for matching of spatio-temporal receptive field responses computed based on the idealized model for spatio-temporal receptive fields according to (30), when complemented by spatial and temporal differentiation according to the theory presented in Lindeberg (2023, 2024c).

Finally, we have in Section 7 considered if we could from the theory predict if the receptive fields of the simple cells and complex cells would have the ability to span similar types of variabilities in receptive field shapes as inferred from the presented theory:

- From existing results, by combining the spans over the degrees of freedom corresponding to uniform scaling transformations and rotations, it appears clear that we could regard the primary visual cortex to be able to be covariant under similarity transformations, that is to combinations of uniform scaling transformations and rotations.
- If we additionally would interpret the potential support in Lindeberg (2024a) for the hypothesis that the receptive field shapes would additionally be expanded over different degrees of elongations, as predicted from the variabilities of the degree of orientation selectivity established from neurophysiological recordings by Nauhaus *et al.* (2008) and Goris *et al.* (2015), it seems natural to also predict that the receptive fields in the primary visual cortex could exhibit properties as would be obtained if the primary visual cortex would have the ability to be covariant also over a significant span over the group of 2-D spatial affine transformations, that is also to image transformations involving non-uniform scaling transformations, as naturally arise from variations of the slant angle, when observing smooth local surface patches in the world from different viewing directions.

To firmly establish if these predictions would hold in reality in the primary visual cortex of higher species, further biological experiments would, however, be extremely valuable, for which explicitly testable experimental hypotheses concerning specific subgroups of 2-D spatial affine transformations have been outlined in Section 3.2.1 in Lindeberg (2023) and Sections 3.2–3.3 in Lindeberg (2024a).

8.1 Outlook

If it could be established that the receptive field shapes in the primary visual cortex would exhibit a variability corresponding to the degrees of freedom in 2-D spatial affine transformations, then such a result would constitute partial support for the working hypothesis that the receptive fields

in the primary visual cortex of higher mammals could be regarded as an affine covariant family of basis functions, that performs an expansion of the incoming image data over the degrees of freedom of 2-D spatial image transformations. A topic of particular interest could also be to investigate if the presence of such covariance properties would be different for different species, and, if so, concerning what species.

Irrespective of such possible biological implications, the theoretical analysis of the degrees of freedom of 2-D spatial affine transformations, with its relations to the degrees of freedom in the affine Gaussian derivative model, is also important for modelling and understanding the computational functions in computer vision systems, that derive information about the environment from dense measurements of image structures or surface patterns from smooth surfaces in the environment.

A Appendix

A.1 Derivation of the decomposition and the parameterization of 2-D spatial affine transformation matrix

A.1.1 Basic definitions

Consider a 2-D spatial affine transformation of the form

$$\mathcal{A} = \begin{pmatrix} a_{11} & a_{12} \\ a_{21} & a_{22} \end{pmatrix} \quad (60)$$

and introduce the following descriptors from the elements a_{ij} of \mathcal{A} :

$$T = \frac{a_{11} + a_{22}}{2}, \quad (61)$$

$$A = \frac{a_{21} - a_{12}}{2}, \quad (62)$$

$$C = \frac{a_{11} - a_{22}}{2}, \quad (63)$$

$$S = \frac{a_{12} + a_{21}}{2}. \quad (64)$$

A.1.2 Product decompositions of the affine transformation matrix

Let us next decompose the affine transformation matrix \mathcal{A} according to a singular value decomposition

$$\mathcal{A} = U \Sigma V^T, \quad (65)$$

where U and V are unitary matrices and Σ a diagonal matrix. Let us, however, next rewrite this decomposition as

$$\mathcal{A} = \mathcal{R}_\alpha \text{diag}(\rho_1, \rho_2) \mathcal{R}_\beta^T, \quad (66)$$

where

$$\mathcal{R}_\alpha = \begin{pmatrix} \cos \alpha & -\sin \alpha \\ \sin \alpha & \cos \alpha \end{pmatrix} \quad (67)$$

and

$$\mathcal{R}_\beta = \begin{pmatrix} \cos \beta & -\sin \beta \\ \sin \beta & \cos \beta \end{pmatrix} \quad (68)$$

are rotation matrices, and $\text{diag}(\rho_1, \rho_2)$ is a diagonal matrix with the elements ρ_1 and ρ_2 .

A.1.3 Relations between the parameters of the product decomposition and the TACS descriptors

By expanding the decomposition (66)

$$\mathcal{A} = \begin{pmatrix} \cos \alpha & -\sin \alpha \\ \sin \alpha & \cos \alpha \end{pmatrix} \begin{pmatrix} \rho_1 & 0 \\ 0 & \rho_2 \end{pmatrix} \begin{pmatrix} \cos \beta & -\sin \beta \\ \sin \beta & \cos \beta \end{pmatrix} \quad (69)$$

and identifying with the elements a_{ij} in (60) we then obtain

$$a_{11} = \rho_1 \cos \alpha \cos \beta + \rho_2 \sin \alpha \sin \beta, \quad (70)$$

$$a_{12} = \rho_1 \cos \alpha \sin \beta - \rho_2 \sin \alpha \cos \beta, \quad (71)$$

$$a_{21} = \rho_1 \sin \alpha \cos \beta - \rho_2 \cos \alpha \sin \beta, \quad (72)$$

$$a_{22} = \rho_1 \sin \alpha \sin \beta + \rho_2 \cos \alpha \cos \beta. \quad (73)$$

By next using the following trigonometric relationships

$$\sin(x+y) = \sin x \cos y + \cos x \sin y, \quad (74)$$

$$\sin(x-y) = \sin x \cos y - \cos x \sin y, \quad (75)$$

$$\cos(x+y) = \cos x \cos y - \sin x \sin y, \quad (76)$$

$$\cos(x-y) = \cos x \cos y + \sin x \sin y, \quad (77)$$

we then obtain that the explicit expressions for the TACS descriptors according to (61)–(64) are given by

$$T = \frac{1}{2} (\rho_1 + \rho_2) \cos(\alpha - \beta), \quad (78)$$

$$A = \frac{1}{2} (\rho_1 + \rho_2) \sin(\alpha - \beta), \quad (79)$$

$$C = \frac{1}{2} (\rho_1 - \rho_2) \cos(\alpha + \beta), \quad (80)$$

$$S = \frac{1}{2} (\rho_1 - \rho_2) \sin(\alpha + \beta). \quad (81)$$

A.1.4 Relationships between the singular values ρ_1 and ρ_2 and the derived PQ descriptors

By further introducing the derived PQ descriptors according to

$$P = \sqrt{T^2 + A^2}, \quad (82)$$

$$Q = \sqrt{C^2 + S^2}, \quad (83)$$

we then obtain that

$$P = \frac{1}{2} |\rho_1 + \rho_2|, \quad (84)$$

$$Q = \frac{1}{2} |\rho_1 - \rho_2|. \quad (85)$$

A.1.5 Explicit expressions for the singular values ρ_1 and ρ_2

For the geometric application we are interested in, we are primarily interested in affine transformation matrices \mathcal{A} that are reasonably close to the unit matrix multiplied by some scalar scaling factor. Therefore, we will assume that both $\rho_1 > 0$ and $\rho_2 > 0$. Additionally, we will for the following parameterizations use the convention to order the singular values such that $\rho_1 > \rho_2$. Then, we obtain

$$P = \frac{1}{2} (\rho_1 + \rho_2), \quad (86)$$

$$Q = \frac{1}{2} (\rho_1 - \rho_2), \quad (87)$$

which in turn gives

$$\rho_1 = P + Q, \quad (88)$$

$$\rho_2 = P - Q. \quad (89)$$

A.1.6 Relationships for the angular parameters α , β , φ and ψ

By combining (78) and (79), we additionally get

$$\frac{A}{T} = \tan(\alpha - \beta), \quad (90)$$

and by combining (80) and (81), we get

$$\frac{S}{C} = \tan(\alpha + \beta). \quad (91)$$

Let us next introduce the new variables

$$\varphi = \alpha - \beta, \quad (92)$$

$$\psi = \alpha + \beta, \quad (93)$$

which correspond to the relationships

$$\alpha = \frac{\psi + \varphi}{2}, \quad (94)$$

$$\beta = \frac{\psi - \varphi}{2}. \quad (95)$$

Then, we obtain the solutions

$$\varphi = \arctan\left(\frac{A}{T}\right) + n_\varphi \pi, \quad (96)$$

$$\psi = \arctan\left(\frac{S}{C}\right) + n_\psi \pi, \quad (97)$$

for some integers n_φ and n_ψ , where we, for the purpose of parameterizing affine transformation matrices \mathcal{A} , prefer to choose the principal solutions according to

$$\varphi = \text{atan2}(A, T), \quad (98)$$

$$\psi = \text{atan2}(S, C), \quad (99)$$

where $\text{atan2}(y, x)$ denotes the function that returns the angle between the positive x -axis and the vector from the origin to the point (x, y) , with the restriction that this angle assumes values in the interval $]-\pi, \pi]$.

A.1.7 Resulting matrix decompositions

From the above explicit expressions for the angles α and β , we then obtain that the decomposition (66) can be written as

$$\begin{aligned} A &= \mathcal{R}_\alpha \text{diag}(\rho_1, \rho_2) \mathcal{R}_\beta^T \\ &= \mathcal{R}_{\frac{\psi+\varphi}{2}} \text{diag}(\rho_1, \rho_2) \mathcal{R}_{\frac{\psi-\varphi}{2}}^T \\ &= \mathcal{R}_{\frac{\psi}{2}} \mathcal{R}_{\frac{\varphi}{2}} \text{diag}(\rho_1, \rho_2) \mathcal{R}_{\frac{\varphi}{2}}^T \mathcal{R}_{\frac{\psi}{2}}^T, \end{aligned} \quad (100)$$

which can also be expressed on the more symmetric form

$$A = \sqrt{\rho_1 \rho_2} \mathcal{R}_{\frac{\psi}{2}} \mathcal{R}_{\frac{\varphi}{2}} \text{diag}\left(\sqrt{\frac{\rho_1}{\rho_2}}, \sqrt{\frac{\rho_2}{\rho_1}}\right) \mathcal{R}_{\frac{\varphi}{2}}^T \mathcal{R}_{-\frac{\psi}{2}}. \quad (101)$$

A.2 Analysis of the proposed decomposition of 2-D affine transformations for special subgroups of affine transformations

In the following, we will compute the parameters in the proposed decomposition of affine transformations according to (101) for four basic classes of image transformations, in terms of uniform scaling transformations, pure rotations and non-uniform scaling transformation.

A.2.1 Uniform scaling transformations

For a uniform scaling transformation with spatial scaling factor $S_x > 0$ and with the corresponding spatial scaling transformation matrix

$$S = \begin{pmatrix} S_x & 0 \\ 0 & S_x \end{pmatrix}, \quad (102)$$

we have

$$T = \frac{a_{11} + a_{22}}{2} = S_x \quad (103)$$

$$A = \frac{a_{21} - a_{12}}{2} = 0, \quad (104)$$

$$C = \frac{a_{11} - a_{22}}{2} = 0, \quad (105)$$

$$S = \frac{a_{12} + a_{21}}{2} = 0, \quad (106)$$

which then gives

$$P = \sqrt{T^2 + A^2} = S_x, \quad (107)$$

$$Q = \sqrt{C^2 + S^2} = 0, \quad (108)$$

$$\rho_1 = P + Q = S_x, \quad (109)$$

$$\rho_2 = P - Q = S_x, \quad (110)$$

$$\varphi = \text{atan2}(A, T) = 0, \quad (111)$$

$$\psi = \text{atan2}(S, C) = \text{undefined}. \quad (112)$$

That the angle ψ is undefined here, means that this angle is formally underdetermined, and that any value of ψ will be consistent with the decomposition (101). Without loss of generality, we can therefore make the simplest choice of $\psi = 0$.

A.2.2 Pure rotations

For a pure rotation with rotation angle γ and the corresponding rotation matrix

$$\mathcal{R} = \begin{pmatrix} \cos \gamma & -\sin \gamma \\ \sin \gamma & \cos \gamma \end{pmatrix}, \quad (113)$$

we have

$$T = \frac{a_{11} + a_{22}}{2} = \cos \gamma, \quad (114)$$

$$A = \frac{a_{21} - a_{12}}{2} = \sin \gamma, \quad (115)$$

$$C = \frac{a_{11} - a_{22}}{2} = 0, \quad (116)$$

$$S = \frac{a_{12} + a_{21}}{2} = 0, \quad (117)$$

which then gives

$$P = \sqrt{T^2 + A^2} = 1, \quad (118)$$

$$Q = \sqrt{C^2 + S^2} = 0, \quad (119)$$

$$\rho_1 = P + Q = 1, \quad (120)$$

$$\rho_2 = P - Q = 1, \quad (121)$$

$$\varphi = \text{atan2}(A, T) = \text{atan2}(\sin \gamma, \cos \gamma) = \gamma \quad (122)$$

$$\psi = \text{atan2}(S, C) = \text{undefined}. \quad (123)$$

Again, since the angle ψ is not formally restricted in the decomposition (101), we make the simplest choice of choosing $\psi = 0$.

A.2.3 Non-uniform scaling transformations

For a non-uniform scaling transformation of the form

$$A = \mathcal{R}_{\frac{\gamma}{2}} \text{diag}(S_1, S_2) \mathcal{R}_{\frac{\gamma}{2}}^T \\ = \begin{pmatrix} \cos \frac{\gamma}{2} & -\sin \frac{\gamma}{2} \\ \sin \frac{\gamma}{2} & \cos \frac{\gamma}{2} \end{pmatrix} \begin{pmatrix} S_1 & 0 \\ 0 & S_2 \end{pmatrix} \begin{pmatrix} \cos \frac{\gamma}{2} & \sin \frac{\gamma}{2} \\ -\sin \frac{\gamma}{2} & \cos \frac{\gamma}{2} \end{pmatrix} \quad (124)$$

with the spatial scaling factors $S_1 > S_2 > 0$ and the orientation $\frac{\gamma}{2}$ of the preferred symmetry axis, we do after a straightforward expansion of the matrix product followed by simplifications get that

$$T = \frac{a_{11} + a_{22}}{2} = \frac{S_1 + S_2}{2}, \quad (125)$$

$$A = \frac{a_{21} - a_{12}}{2} = 0, \quad (126)$$

$$C = \frac{a_{11} - a_{22}}{2} = \frac{(S_1 - S_2)}{2} \cos \gamma, \quad (127)$$

$$S = \frac{a_{12} + a_{21}}{2} = \frac{(S_1 - S_2)}{2} \sin \gamma, \quad (128)$$

which then gives

$$P = \sqrt{T^2 + A^2} = \frac{S_1 + S_2}{2}, \quad (129)$$

$$Q = \sqrt{C^2 + S^2} = \frac{|S_1 - S_2|}{2} = \frac{S_1 - S_2}{2}, \quad (130)$$

$$\rho_1 = P + Q = S_1, \quad (131)$$

$$\rho_2 = P - Q = S_2, \quad (132)$$

$$\varphi = \text{atan2}(A, T) = 0, \quad (133)$$

$$\psi = \text{atan2}(S, C) = \text{atan2}(\sin \gamma, \cos \gamma) = \gamma. \quad (134)$$

In this respect, the proposed sign conventions for the singular values ρ_1 and ρ_2 , as well as the choices for determining the angle ψ , correctly recover the parameters in the original non-uniform transformation of the form (124).

A.2.4 Pure skewing transformations

Consider a pure skewing transformation with skewing angle γ of the form

$$x' = x + y \tan \gamma, \quad (135)$$

$$y' = y, \quad (136)$$

that is with an affine transformation matrix of the form

$$\mathcal{A} = \begin{pmatrix} 1 & \tan \gamma \\ 0 & 1 \end{pmatrix}, \quad (137)$$

we have

$$T = \frac{a_{11} + a_{22}}{2} = 1, \quad (138)$$

$$A = \frac{a_{21} - a_{12}}{2} = -\frac{\tan \gamma}{2}, \quad (139)$$

$$C = \frac{a_{11} - a_{22}}{2} = 0, \quad (140)$$

$$S = \frac{a_{12} + a_{21}}{2} = -\frac{\tan \gamma}{2}, \quad (141)$$

which then gives

$$P = \sqrt{T^2 + A^2} = \sqrt{1 + \frac{\tan^2 \gamma}{4}}, \quad (142)$$

$$Q = \sqrt{C^2 + S^2} = \frac{|\tan \gamma|}{2}, \quad (143)$$

$$\rho_1 = P + Q = \sqrt{1 + \frac{\tan^2 \gamma}{4}} + \frac{|\tan \gamma|}{2}, \quad (144)$$

$$\rho_2 = P - Q = \sqrt{1 + \frac{\tan^2 \gamma}{4}} - \frac{|\tan \gamma|}{2}, \quad (145)$$

$$\varphi = \text{atan2}(A, T) = \text{atan2}\left(-\frac{\tan \gamma}{2}, 1\right) = \arctan\left(-\frac{\tan \gamma}{2}\right), \quad (146)$$

$$\psi = \text{atan2}(S, C) = \text{atan2}\left(-\frac{\tan \gamma}{2}, 0\right) = -\frac{\pi}{2} \text{ sign } \gamma. \quad (147)$$

In other words, according to the proposed decomposition (101) of affine image transformations, a pure skewing transformation is regarded as a more complex image transformation, that corresponds to (i) first rotating the input image to a preferred symmetry orientation in the image plane by the angle $-\frac{\psi}{2}$, then (ii) rotating the image by the angle $\frac{\psi}{2}$ before (iii) performing a pure non-uniform scaling transformation with the spatial scaling factors ρ_1 and ρ_2 , after which the image is again (iv) rotated by the same angle $\frac{\psi}{2}$, before finally being (vi) rotated back from the preferred symmetry orientation.

Statements and declarations

Competing interests

The author declares no competing interests.

References

- J. Aczél, Z. Boros, J. Heller, and C.-T. Ng. Functional equations in binocular space perception. *Journal of Mathematical Psychology*, 43(1):71–101, 1999.
- G. Benvenuti, Y. Chen, C. Ramakrishnan, K. Deisseroth, W. S. Geisler, and E. Seidemann. Scale-invariant visual capabilities explained by topographic representations of luminance and texture in primate V1. *Neuron*, 100(6):1504–1512, 2018.
- K. Beshkov and G. G. T. Einevoll. Topological structure of population activity in mouse visual cortex encodes visual scene rotations. *bioRxiv*, 2023.02.13.528247, 2023.
- I. Biederman and E. E. Cooper. Size invariance in visual object priming. *Journal of Experimental Psychology: Human Perception and Performance*, 18(1):121–133, 1992.
- G. G. Blasdel. Orientation selectivity, preference and continuity in monkey striate cortex. *Journal of Neuroscience*, 12(8):3139–3161, 1992.
- T. Bonhoeffer and A. Grinvald. Iso-orientation domains in cat visual cortex are arranged in pinwheel-like patterns. *Nature*, 353:429–431, 1991.
- B. R. Conway and M. S. Livingstone. Spatial and temporal properties of cone signals in alert macaque primary visual cortex. *Journal of Neuroscience*, 26(42):10826–10846, 2006.
- A. De and G. D. Horwitz. Spatial receptive field structure of double-opponent cells in macaque V1. *Journal of Neurophysiology*, 125(3):843–857, 2021.
- G. C. DeAngelis and A. Anzai. A modern view of the classical receptive field: Linear and non-linear spatio-temporal processing by

- V1 neurons. In L. M. Chalupa and J. S. Werner, editors, *The Visual Neurosciences*, volume 1, pages 704–719. MIT Press, 2004.
- G. C. DeAngelis, I. Ohzawa, and R. D. Freeman. Receptive field dynamics in the central visual pathways. *Trends in Neuroscience*, 18(10):451–457, 1995.
- J. J. DiCarlo, D. Zoccolan, and N. C. Rust. How does the brain solve visual object recognition? *Neuron*, 73(3):415–434, 2012.
- O. Faugeras. *Three-Dimensional Computer Vision*. MIT Press, Cambridge, Massachusetts, 1993.
- C. S. Furfanski and S. A. Engel. Perceptual learning in object recognition: Object specificity and size invariance. *Vision Research*, 40:473–484, 2000.
- J. Gårding and T. Lindeberg. Direct estimation of local surface shape in a fixating binocular vision system. In J.-O. Eklundh, editor, *Proc. European Conf. on Computer Vision (ECCV'94)*, volume 800 of *Lecture Notes in Computer Science*, pages 365–376, Stockholm, Sweden, May, 1994. Springer-Verlag.
- J. Gårding and T. Lindeberg. Direct computation of shape cues using scale-adapted spatial derivative operators. *International Journal of Computer Vision*, 17(2):163–191, 1996.
- M. A. Georgeson, K. A. May, T. C. A. Freeman, and G. S. Hesse. From filters to features: Scale-space analysis of edge and blur coding in human vision. *Journal of Vision*, 7(13):7.1–21, 2007.
- M. Ghodrati, S.-M. Khaligh-Razavi, and S. R. Lehky. Towards building a more complex view of the lateral geniculate nucleus: Recent advances in understanding its role. *Progress in Neurobiology*, 156:214–255, 2017.
- R. L. T. Goris, E. P. Simoncelli, and J. A. Movshon. Origin and function of tuning diversity in Macaque visual cortex. *Neuron*, 88(4):819–831, 2015.
- Y. Han, G. Roig, G. Geiger, and T. Poggio. Scale and translation-invariance for novel objects in human vision. *Scientific Reports*, 10(1):1411, 2020.
- M. Hansard and R. Horaud. Cyclopean geometry of binocular vision. *Journal of the Optical Society of America A*, 25(9):2357–2369, 2008.
- T. Hansen and H. Neumann. A recurrent model of contour integration in primary visual cortex. *Journal of Vision*, 8(8):8.1–25, 2008.
- R. Hartley and A. Zisserman. *Multiple View Geometry in Computer Vision*. Cambridge University Press, 2004. Second Edition.
- G. S. Hesse and M. A. Georgeson. Edges and bars: where do people see features in 1-D images? *Vision Research*, 45(4):507–525, 2005.
- C. P. Hung, G. Kreiman, T. Poggio, and J. J. DiCarlo. Fast readout of object identity from macaque inferior temporal cortex. *Science*, 310:863–866, 2005.
- L. Isik, E. M. Meyers, J. Z. Leibo, and T. Poggio. The dynamics of invariant object recognition in the human visual system. *Journal of Neurophysiology*, 111(1):91–102, 2013.
- M. Ito, H. Tamura, I. Fujita, and K. Tanaka. Size and position invariance of neuronal responses in monkey inferotemporal cortex. *Journal of Neurophysiology*, 73(1):218–226, 1995.
- E. N. Johnson, M. J. Hawken, and R. Shapley. The orientation selectivity of color-responsive neurons in Macaque V1. *The Journal of Neuroscience*, 28(32):8096–8106, 2008.
- D. G. Jones and J. Malik. A computational framework for determining stereo correspondences from a set of linear spatial filters. In G. Sandini, editor, *Proc. European Conf. on Computer Vision (ECCV'92)*, volume 588 of *Lecture Notes in Computer Science*, pages 395–410, Santa Margherita Ligure, Italy, May, 1992. Springer-Verlag.
- J. Jones and L. Palmer. The two-dimensional spatial structure of simple receptive fields in cat striate cortex. *J. of Neurophysiology*, 58:1187–1211, 1987a.
- J. Jones and L. Palmer. An evaluation of the two-dimensional Gabor filter model of simple receptive fields in cat striate cortex. *J. of Neurophysiology*, 58:1233–1258, 1987b.
- E. Koch, J. Jin, J. M. Alonso, and Q. Zaidi. Functional implications of orientation maps in primary visual cortex. *Nature Communications*, 7(1):13529, 2016.
- J. J. Koenderink. The structure of images. *Biological Cybernetics*, 50(5):363–370, 1984.
- J. J. Koenderink and A. J. van Doorn. Geometry of binocular vision and a model for stereopsis. *Biological Cybernetics*, 21(1):29–35, 1976.
- J. J. Koenderink and A. J. van Doorn. Representation of local geometry in the visual system. *Biological Cybernetics*, 55(6):367–375, 1987.
- J. J. Koenderink and A. J. van Doorn. Generic neighborhood operators. *IEEE Transactions on Pattern Analysis and Machine Intelligence*, 14(6):597–605, Jun, 1992.
- T. Lindeberg. *Scale-Space Theory in Computer Vision*. Springer, 1993.
- T. Lindeberg. Direct estimation of affine deformations of brightness patterns using visual front-end operators with automatic scale selection. In *Proc. International Conference on Computer Vision (ICCV'95)*, pages 134–141, Cambridge, MA, Jun, 1995.
- T. Lindeberg. A computational theory of visual receptive fields. *Biological Cybernetics*, 107(6):589–635, 2013a.
- T. Lindeberg. Invariance of visual operations at the level of receptive fields. *PLOS ONE*, 8(7):e66990, 2013b.
- T. Lindeberg. Normative theory of visual receptive fields. *Heliyon*, 7(1):e05897:1–20, 2021. doi: 10.1016/j.heliyon.2021.e05897.
- T. Lindeberg. Covariance properties under natural image transformations for the generalized Gaussian derivative model for visual receptive fields. *Frontiers in Computational Neuroscience*, 17:1189949:1–23, 2023.
- T. Lindeberg. Do the receptive fields in the primary visual cortex span a variability over the degree of elongation of the receptive fields? *arXiv preprint arXiv:2404.04858*, 2024a.
- T. Lindeberg. Orientation selectivity properties for the affine Gaussian derivative and the affine Gabor models for visual receptive fields. *arXiv preprint arXiv:2304.11920*, 2024b.
- T. Lindeberg. Unified theory for joint covariance properties under geometric image transformations for spatio-temporal receptive fields according to the generalized Gaussian derivative model for visual receptive fields. *arXiv preprint arXiv:2311.10543*, 2024c.
- T. Lindeberg and J. Gårding. Shape-adapted smoothing in estimation of 3-D shape cues from affine distortions of local 2-D structure. *Image and Vision Computing*, 15(6):415–434, 1997.
- N. K. Logothetis, J. Pauls, and T. Poggio. Shape representation in the inferior temporal cortex of monkeys. *Current Biology*, 5(2):552–563, 1995.
- D. G. Lowe. Towards a computational model for object recognition in IT cortex. In *Biologically Motivated Computer Vision*, volume 1811 of *Springer LNCS*, pages 20–31. Springer, 2000.
- S. Marcelja. Mathematical description of the responses of simple cortical cells. *Journal of Optical Society of America*, 70(11):1297–1300, 1980.
- K. A. May and M. A. Georgeson. Blurred edges look faint, and faint edges look sharp: The effect of a gradient threshold in a multi-scale edge coding model. *Vision Research*, 47(13):1705–1720, 2007.
- A. Mitiche and J.-M. Létang. Stereokinematic analysis of visual data in active convergent stereoscopy. *Robotics and Autonomous systems*, 25(1-2):43–71, 1998.
- N. A. R. Murty and S. P. Arun. A balanced comparison of object invariances in monkey IT neurons. *eNeuro*, 4(2), 2017.
- I. Nauhaus, A. Benucci, M. Carandini, and D. L. Ringach. Neuronal selectivity and local map structure in visual cortex. *Neuron*, 57(5):673–679, 2008.
- Z.-J. Pei, G.-X. Gao, B. Hao, Q.-L. Qiao, and H.-J. Ai. A cascade model of information processing and encoding for retinal prosthesis. *Neural Regeneration Research*, 11(4):646, 2016.
- T. A. Poggio and F. Anselmi. *Visual Cortex and Deep Networks: Learning Invariant Representations*. MIT Press, 2016.

- M. Porat and Y. Y. Zeevi. The generalized Gabor scheme of image representation in biological and machine vision. *IEEE Transactions on Pattern Analysis and Machine Intelligence*, 10(4):452–468, 1988.
- D. L. Ringach. Spatial structure and symmetry of simple-cell receptive fields in macaque primary visual cortex. *Journal of Neurophysiology*, 88:455–463, 2002.
- D. L. Ringach. Mapping receptive fields in primary visual cortex. *Journal of Physiology*, 558(3):717–728, 2004.
- J. Turski. On binocular vision: The geometric horopter and Cyclopean eye. *Vision Research*, 119:73–81, 2016.
- J. Turski. New results in stereopsis and Listings law. *Scientific Reports*, 14(1):22474, 2024.
- T. Uka and G. C. DeAngelis. Binocular vision: An orientation to disparity coding. *Current Biology*, 12(22):R764–R766, 2002.
- E. Y. Walker, F. H. Sinz, E. Cobos, T. Muhammad, E. Froudarakis, P. G. Fahey, A. S. Ecker, J. Reimer, X. Pitkow, and A. S. Tolias. Inception loops discover what excites neurons most using deep predictive models. *Nature Neuroscience*, 22(12):2060–2065, 2019.
- S. A. Wallis and M. A. Georgeson. Mach edges: Local features predicted by 3rd derivative spatial filtering. *Vision Research*, 49(14):1886–1893, 2009.
- Q. Wang and M. W. Spratling. Contour detection in colour images using a neurophysiologically inspired model. *Cognitive Computation*, 8(6):1027–1035, 2016.
- L. Wiskott. How does our visual system achieve shift and size invariance? In J. L. van Hemmen and T. J. Sejnowski, editors, *Problems in Systems Neuroscience*, volume 23, pages 322–340. Oxford Academic, 2006.
- R. A. Young. The Gaussian derivative model for spatial vision: I. Retinal mechanisms. *Spatial Vision*, 2(4):273–293, 1987.
- R. A. Young and R. M. Lesperance. The Gaussian derivative model for spatio-temporal vision: II. Cortical data. *Spatial Vision*, 14(3, 4):321–389, 2001.
- R. A. Young, R. M. Lesperance, and W. W. Meyer. The Gaussian derivative model for spatio-temporal vision: I. Cortical model. *Spatial Vision*, 14(3, 4):261–319, 2001.